

行政院國家科學委員會專題研究計畫 期中進度報告

垂直圓柱容器中向下強制氣流流過一水平加熱晶圓之渦旋
流結構與相關熱傳特性研究(2/3)

計畫類別：個別型計畫

計畫編號：NSC91-2212-E-009-042-

執行期間：91年08月01日至92年07月31日

執行單位：國立交通大學機械工程研究所

計畫主持人：林清發

報告類型：精簡報告

報告附件：出席國際會議研究心得報告及發表論文

處理方式：本計畫可公開查詢

中 華 民 國 92 年 5 月 23 日

出席國際會議心得報告

本人於民國 91 年 8 月 18 日至 23 日受邀出席於法國 Grenoble 舉行的第十二屆國際熱傳會議(Twelfth International Heat Transfer Conference)，發表一篇 Keynote Lecture，講題是「Buoyancy Driven Vortex Flow and Thermal Structures in a Very Low Reynolds number Mixed Convective Gas Flow through a Horizontal Channel」。此一國際熱傳會議每四年舉辦一次，此屆會議共邀請了 34 個 Keynote Lectures，發表 515 篇 Technical Papers，內容及範圍涵蓋極廣，幾乎所有之熱傳研究領域都有，包括基本研究和工業應用。

在 Keynote Lectures 的部分，包含有 Microscale, MEMS & Nanoscale Heat Transfer, Thermal Radiation, Turbulent Flow (Wall Function), Boiling and Two Phase Heat Transfer, Heat Transfer Enhancement & Heat Exchanger (Flow Induced vibration and Noise), Natural and Mixed Convection, Cryogenic Heat and Mass Transfer (Biomedical Applications), Laser Interferometry for Local Heat Flux Measurement 非牛頓流體熱傳, 工廠設計(最佳熱傳和流體模擬), Heat Pump & Refrigeration Systems, 燃料電池熱流及高溫太陽能等。這些研究主題都是目前很受各國學者所重視，可作為國內相關學者參考。

至於 Technical Papers 的部分則區分為 Single Phase 和 Two Phase Heat Transfer, Local Thermal Non-Equilibrium 熱傳(Nano systems, Radiation, Fluids and Solids), Nonhomogeneous Media 熱傳(Drying, Heat and Mass Transfer, Melting, Freezing, Solidification, Reacting Media, Porous Media 與 Convection), Engineering Systems 熱傳(? 相 Heat Exchangers, Finned Systems. Optimization, Turbomachinery and Gas Turbines, High Temperature Processes, Manufacturing Processes, Innovative Heat Exchangers, Heat Pipes, Refrigeration, 核工, 熱交換器, Cryogenics, 熱物理性質, Electrical and Electronic Devices, Ribs and Turbulence Promoters, Alternative Energy Production 與 Contact Resistance), 幾乎包括所有傳統和最近的熱傳研究領域。
附件三：最近比較熱門的研究方向則是微奈米熱傳、微機電製程與元件熱傳、生物製藥及人體相關熱流、燃料電池與半導體製程相關熱流等之研究。

Buoyancy driven vortex flow and thermal structures in a very low Reynolds number mixed convective gas flow through a horizontal channel

Tsing-Fa Lin

Department of Mechanical Engineering, Nation Chiao Tung University 1001 Ta Hsueh Road Hsinchu, Taiwan, R.O.C.

Abstract

This paper starts with an overview of the buoyancy driven vortex flow and associated thermal characteristics in low Reynolds number mixed convection of gas through a bottom heated horizontal plane channel. Various vortex flow patterns reported in the past decades from theoretical, experimental and numerical explorations are examined, including the longitudinal, transverse and mixed vortex rolls. The mixed vortex rolls exist in several forms

and result from the merging and/or splitting of the longitudinal and transverse rolls which are simultaneously present in certain parameter ranges.

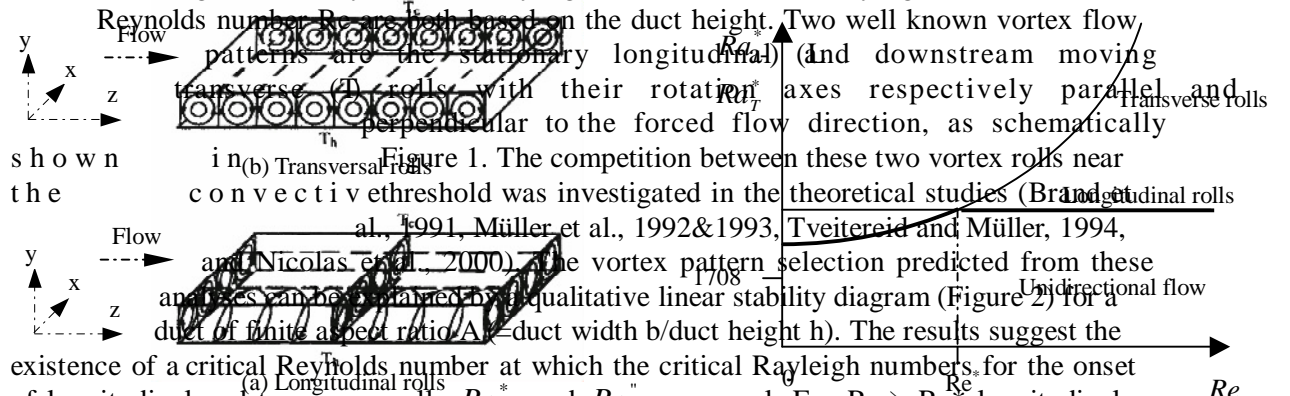
Then, the buoyancy induced formation of the longitudinal and transverse vortex flows from the unidirectional forced convection dominated flow in the channel is illustrated. Besides, the vortex flow affected by the aspect ratio of the channel is also discussed. Moreover, the stabilization of the unstable vortex flow driven at very high buoyancy-to-inertia ratios through the top plate inclination, top plate heating and a ~~surface~~ surface mounted rib is inspected. Furthermore, our recent results for the mixed convective vortex flow structures over a heated circular substrate are presented. Finally, directions for future research ~~pointed~~ pointed out according to the need for thin film vapor phase epitaxy frequently used in microelectronic fabrication.

1. Introduction

The buoyancy driven vortex flow and the associated thermal characteristics in a very low Reynolds number mixed convective flow of gas through a horizontal plane channel uniformly heated from below and cooled from above have been extensively investigated in the past two decades because the important roles they play in growing high quality thin crystal films from metal organic chemical vapor deposition (MOCVD) in microelectronic fabrication of optical-electronic devices (Hitchman and Jensen 1993). Many complex vortex flow structures including return flow, longitudinal, transverse and mixed rolls were revealed from the theoretical, numerical and experimental explorations. This article starts with an overview of this vortex gas flow. In particular, the flow regime map and some important characteristics of the vortex flow patterns are to be examined. Quantitative data for the appearance of the vortex flow patterns and some flow features will be reviewed. Besides, how different vortex flow structures form from the unidirectional forced convective flow and the effects of the duct aspect ratio will be discussed. Moreover, the possible flow stabilization by the top plate inclination, top plate heating and a surface mounted rib will be inspected. Additionally, the vortex flow patterns driven by a circular heated substrate are illustrated. Finally, directions for future research will be pointed out.

2. Overview of vortex flow in horizontal plane channel

In a very low Reynolds number mixed convective flow through a bottom heated horizontal plane channel ($Re \leq 100$) many widely different vortex flow patterns were predicted from theoretical linear stability and weak nonlinear analyses at the onset of Rayleigh-Bénard convection. Similar investigations were conducted in a number of experimental studies over much wider ranges of the Reynolds and Rayleigh numbers. Here the Rayleigh number Ra and



Reynolds number Re are both based on the duct height. Two well known vortex flow patterns are the stationary longitudinal (and downstream moving transverse (T) rolls, with their rotation axes respectively parallel and perpendicular to the forced flow direction, as schematically shown in Figure 1. The competition between these two vortex rolls near the convective threshold was investigated in the theoretical studies (Brandt et al., 1991, Müller et al., 1992 & 1993, Tveitereid and Müller, 1994, and Nicolas et al., 2000). The vortex pattern selection predicted from these analyses can be obtained by a qualitative linear stability diagram (Figure 2) for a duct of finite aspect ratio A (=duct width b /duct height h). The results suggest the existence of a critical Reynolds number at which the critical Rayleigh numbers, for the onset of longitudinal and transverse rolls, Ra_L^* and Ra_T^* are equal. For $Re > Re^*$ longitudinal disturbances become unstable first at Ra_L^* . While for $Re < Re^*$ transverse rolls can be initiated a slightly lower Rayleigh number with $Ra_T^* < Ra_L^*$. Moreover, Ra_L^* does not change with the Reynolds and Prandtl numbers but increases mildly at decreasing duct aspect ratio (Nicolas et al., 2000). However, Ra_T^* increases to some degree with the Reynolds and Prandtl numbers. Besides, Re^* was found to be lower for a higher Prandtl number fluid. For the limiting case of $A \rightarrow \infty$, Re^* is equal to zero and the longitudinal instability always sets in first.

To delineate the vortex patterns in the channel, detailed experimental flow visualization was conducted in several studies covering wide ranges of the governing parameters. Specifically, Chiu and Rosenberger (1987) proposed a flow regime map for nitrogen ($A=10$) locating the boundaries among the flow with no rolls, steady and unsteady rolls. Slightly later, Ouazzani et al. (1989) included the longitudinal and transverse rolls in their map for air ($A=19.5$). Recently, other vortex flow patterns were identified by Lir et al. (2001) and Cheng et al. (2001), as noted from their map for air with $A=16$ and $Re \leq 5$ shown in Figure 3. More specifically, depending on the magnitudes of Re and Ra the flow can consist of the mixed longitudinal and transverse rolls, U-rolls, nonperiodic transverse waves and longitudinal rolls, and inlet stationary transverse rolls and downstream longitudinal rolls, in addition to the regular and irregular longitudinal rolls and transverse rolls. The planform of these vortex patterns can be clearly seen from the top view flow photos given in Figure 4. Note that even at subcritical buoyancy longitudinal rolls along with traversing transverse waves can be induced in the duct.

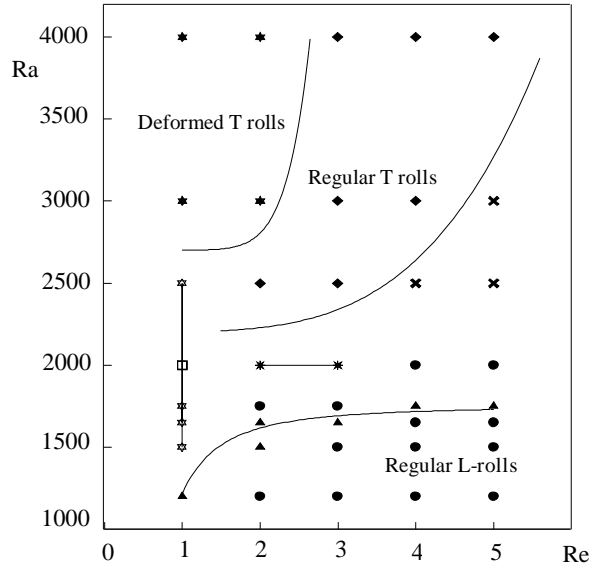


Fig. 3 Flow regime map for different vortex flow patterns observed in flow visualization for air with $A=16$. (○ : T rolls, ◆ : deformed T rolls, * : L rolls, ● : Mixed L & T rolls, × : U rolls, □ : Rectangular rolls, ⊕ : Mixed L & T rolls & downstream irregular cells, ⊗ : Nonperiodic waves & L rolls, ⊙ : Inlet stationary T rolls & downstream L rolls)

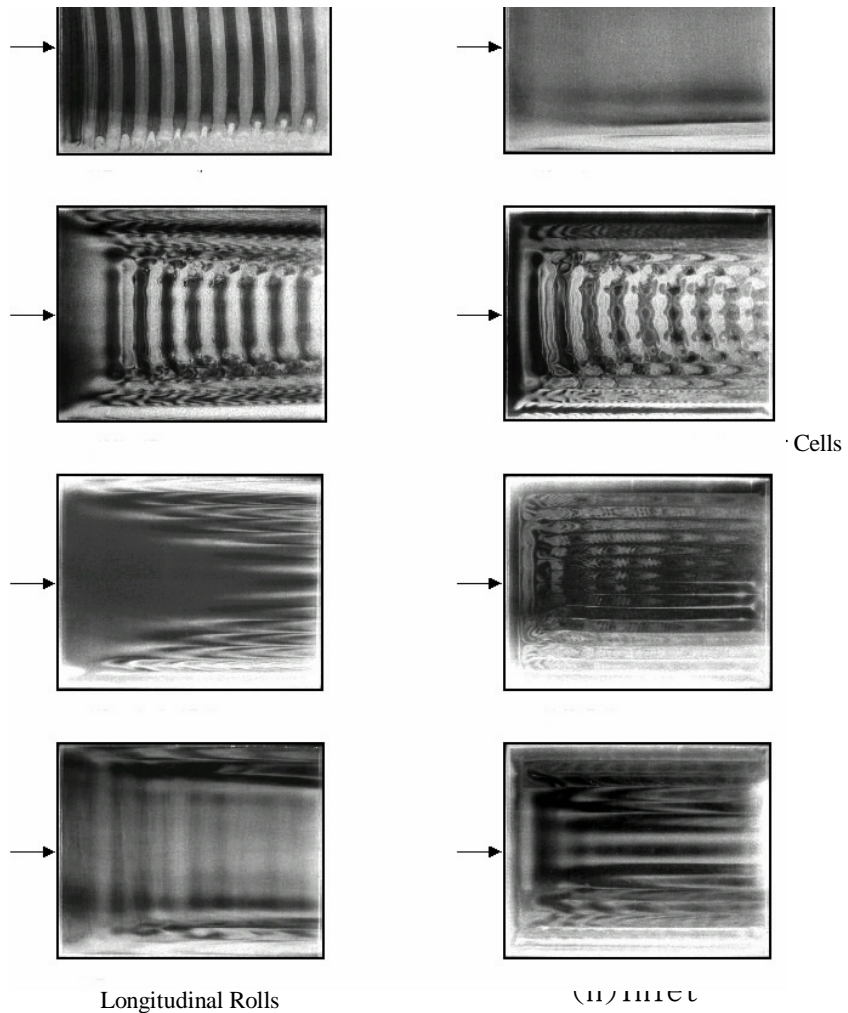


Fig. 4 Top view flow photos at steady or statistical state for $Re=5.0$ and $Ra=$ (a) 4000, (b) 2500, (c) 2000, (d) 1750, (e) 1500, (f) $Re=2.0$ & $Ra=2000$, (g) $Re=1.0$ & $Ra=2000$, and (h) $Re=1.0$ & $Ra=1200$ for air with $A=16$

2.1 Longitudinal rolls

It is well known that in real situation a certain finite traveling distance is needed for the gas flow entering the bottom heated duct to accumulate enough thermal energy to form longitudinal vortex rolls. This onset distance is apparently shorter for higher Rayleigh and/or lower Reynolds numbers. This is equivalent to say that the critical Rayleigh number Ra_c for the onset of L-rolls decreases in the downstream direction. Kamotani et al. (1979) compared their measured data for Ra_c with these computed by the linear stability analysis (Hwang and Cheng (1973)). They noted that the critical Rayleigh number from the experimental measurement was about two-order-of-magnitude higher than that from the stability analysis. At this point we should mention that the critical Rayleigh number Ra_L^* for L-rolls shown in Figure 2 is in fact the value for Ra_c at the far downstream location in a long channel where Ra_c has already leveled off. Moreover, the onset location of each L-roll also depends on its spanwise position in the duct, as clear from Figure 4 (c). Closer to the sidewalls of the channel, the rolls are induced in a shorter axial distance. An empirical correlation for the onset of L-rolls considering the axial and spanwise locations of the air flow was provided by Lir et al. (2001) and it is expressed as

$$\ln Ra_z \approx 11.88 - 0.0367 \cdot x^2 + 0.471 Re_z^{0.5} \quad (1)$$

Here Re_z and Ra_z are respectively the Reynolds and Rayleigh numbers based on the axial distance z , and x is the nondimensional lateral coordinate scaled with the duct height. The average axial distance for the onset of L-rolls was measured by Chiu and Rosenberger (1987) for N_2 with $A \approx 10$. Their data were correlated as

$$Z_c = 0.65 \cdot Re^{0.76} \cdot \left(\frac{Ra - Ra_{\infty}}{Ra_{\infty}} \right)^{-0.44} \quad (2)$$

where $Ra_{\infty} = 1708$ is the critical Rayleigh number for the onset of Rayleigh convection.

Considerable effort has been devoted to exploring the characteristics of longitudinal vortex flow of gas through the experimental flow visualization and velocity and temperature measurement (Ostrach and Kamotani 1975, Kamotani and Ostrach 1976, Kamotani et al. 1979, Hwang and Liu, 1976, Fukui et al., 1983, Chiu and Rosenberger, 1987, Ouazzani et al., 1989, and Chang et al. 1997a). The results from these studies indicate that the rolls, immediately after their onset, grow quickly as the flow in the rolls moves spirally forwards in the downstream direction (Figure 4(c)). When the channel is long enough, the rolls evolve rapidly to a fully developed state. The measured fully developed length z_{fd} was correlated as (Chiu and Rosenberger, 1987)

$$z_{fd} \approx 0.68 \cdot Re^{0.96} \cdot \left(\frac{Ra - Ra_{\infty}}{Ra_{\infty}} \right)^{-0.69} \quad (3)$$

At low buoyancy to inertia ratio Gr/Re^2 , steady and regular longitudinal rolls prevail in the duct. Here Gr is the Grashof number based on duct height. They are spanwise symmetric with respect to the vertical meridional plane. All the fully developed L-rolls have the same size with their diameter equal to the channel height. At certain high Gr/Re^2 the longitudinal vortex flow becomes unsteady and some L-rolls split in one period of time and later merge of L-rolls occurs. These roll splitting and merging processes repeat nonperiodically. The results (Chang et al., 1997a) for air with $A=12$ is illustrated in Figure 5 by showing the flow photos

and schematically sketched cross plane recirculating flow at a selected cross section for several instants of time. One roll splits into three rolls in the period of τ (dimensionless time) from 45 to 51. Thus, two additional rolls appear in the duct. Later for $72 < \tau < 78$ merging of three rolls into one roll occurs. In these two periods all the rolls adjust their sizes. Hence well before the splitting and well after the merging, all the L-rolls have the same size. At even higher buoyancy, we also have generation of few rolls in the duct. Chang et al. (1997a) provided an empirical equation for the onset of unsteady L-rolls and it is

$$z_{us} \approx 13.8 \left(\frac{Re^{1.4}}{Ra} \right)^{0.7} \quad (4)$$

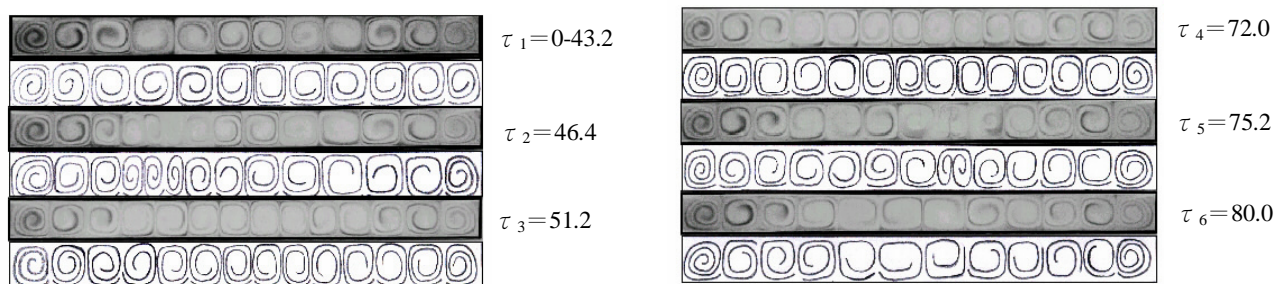


Fig. 5. The cross plane longitudinal vortex flow at selected time instants at crosssection $z=12.62$ showing (a) the roll splitting and (b) roll merging for $Re = 20$ and $Ra = 6000$ for air with $A=12$ ($\tau = t/(d/W_m)$)

According to the transient temperature measurement of the vortex air flow with $A=12$ (Chang et al., 1997), the transition from steady to unsteady states in the longitudinal vortex flow is subcritical, suggesting an abrupt change of a steady flow to a nonperiodic time dependent flow for a very small raise of the buoyancy-to-inertia ratio.

In the past two decades extensive numerical simulation was carried out to investigate the longitudinal vortex flow of gas through solving the steady three dimensional parabolized continuity, Navier-stokes and energy equations (Abou-Ellail and Morcos, 1983, Moffat and Jensen, 1986, Maughan and Incropera, 1990a, and Narusawa, 1993). Besides, unsteady elliptic flow computation was conducted by spall (1996) and Yu et al(1997a). Their results are in good agreement with the experimental data. Moreover, they provide the local Nusselt number distributions which are rather difficult to measure experimentally along the isothermal bottom and top plates of the duct.

2.2 Transverse rolls

Unlike the L-rolls, the downstream moving transverse vortex gas rolls are less studied since they only appear at relatively low Reynolds numbers for $Re < 8$ (Figure 3) and the flow is difficult to control experimentally within a reasonable accuracy. The regular transverse vortex

flow (Figure 4(a)) is mainly characterized by the roll size (wavelength), convection speed of the rolls W_r and oscillation frequency of the flow f . The experimental observation from Luijckx et al. (1981,1982), Ouazzani et al. (1989), Chang and Lin (1996), and Yu et al. (1997b) reveals that all the regular T-rolls have the same diameter which is nearly equal to the channel height. The effects of the Reynolds and Rayleigh numbers on the roll size are relatively mild. Besides, the Trolls travel downstream at the same speed. But this speed is directly proportional to the mean speed of the flow W_m forced into the channel. The effects of the Rayleigh number are small. The roll convection speed for air flow proposed by Ouazzani et al. (1989) is

$$\frac{W_r}{W_m} = 1.50 - 2.7 \times 10^{-5} \cdot Ra \quad (5)$$

The data again for air from Chang and Lin (1996), however, give

$$\frac{W_r}{W_m} \approx 1.30 \quad (6)$$

Note that the regular transverse vortex flow normally oscillates periodically in time. The air temperature variations with time measured by Chang and Lin (1996) indicate that the entire flow oscillates at the same frequency and amplitude. Their measured oscillation frequency of the flow is nearly proportional to the Reynolds number of the flow and is correlated as

$$\frac{f}{\alpha/d^2} \approx 0.47 \cdot Re + 8.864 \times 10^{-5} \cdot Re^3 \quad (7)$$

here α is the thermal diffusivity of the gas. At certain high buoyancy-to-inertia ratio the T-rolls become deformed and the roll deformation is more severe at higher Gr/Re . The structure of T-rolls is completely destroyed at sufficiently high Gr/Re^2 .

At this point it is of interest to unveil how the Trolls are generated in the mixed convective flow of gas in the channel. For this purpose side view flow photos taken at the central vertical plane midway between the duct sides observed by Yu et al. (1997) at consecutive time instants in a typical periodic cycle are shown in Figure 6. The results suggest that at a high buoyancy-to-inertia ratio for $Gr/Re^2 > 35$ an axially slender return flow zone appears in the upstream section of the channel and the buoyancy driven spanwisely elongated thermal from the bottom plate in this upstream section gradually severs the downstream tip of the return flow zone and finally a T-roll forms. After hitting the top plate, the thermal forms another counter-rotating T-roll. Thus, a new pair of T-rolls is generated in the duct entry.

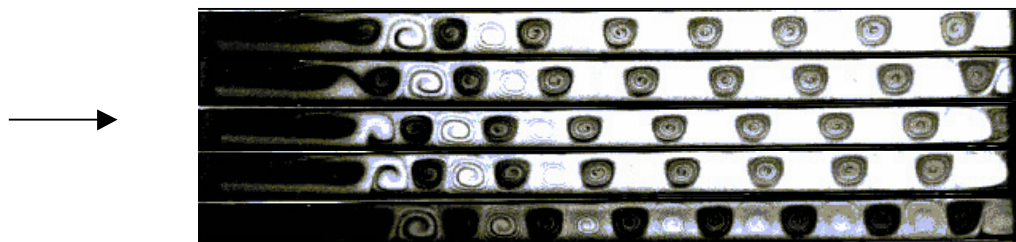


Fig .6 Mid-span ($x= A/2$) side view of the vortex flow showing the formation processes of transverse rolls at selected time instants (a) $t = 0$ s, (b) $t = 2.5$ s, (c) $t = 5.0$ s, (d) $t = 6.2$ s and (e) $t = 7.4$ s for $Re=5.0$ and $Ra = 4000$ for air with $A=12$

It is well known that the appearance of the return flow in the channel will result in some detrimental effects on the high quality thin crystal films grown from MOCVD processes. Hence the return flow has been extensively studied in recent years. Based on flow visualization and/or numerical calculations, various criteria were proposed to delineate the condition for the appearance of the return flow. Visser et al. (1989) proposed that no return flow occurred if

$$\frac{Gr}{Re^k} < \beta_{crit} \quad (8)$$

here $k=1$ for $Re \leq 4$ and $k=2$ for $Re \geq 8$. But β_{crit} varies drastically with the temperature difference between the inlet gas and heated plate, and it ranges from 80 to 160. The criterion from Ingle and Mountziaris (1994) is simpler and is read as

$$\frac{Gr}{Re} < 100 \quad \text{for } 10^{-3} < Re \leq 4 \quad \text{and} \quad Gr/Re^2 < 25 \quad \text{for } 4 \leq Re < 100 \quad (9)$$

The onset of the return flow in a long horizontal CVD reactor was also examined by Makhviladze and Martjushenko (1998). Through a 3D numerical simulation, Ouazzani and Rosenberger (1990) showed that even at a highly subcritical buoyancy the reverse flow in a horizontal MOCVD reactor could be very strong.

2.3 Mixed rolls

In addition to the regular longitudinal and transverse rolls examined above, several mixed vortex flow patterns have been identified in which the Δ and Trolls are simultaneously present in various portions of the channel. A few of these can be seen from the experimental flow photos in Figure 4. Particularly, Figure 4(b) shows a mixed vortex flow consisting of stationary L-rolls near the duct sides and time periodic moving Trolls in the duct core. Note that the Trolls degenerate into weak transverse waves at a lower buoyancy (Figure 4(d)). At lower Re and Ra the downstream Trolls gradually split into recirculating cells (Figure 4(f)). Moreover, we can have stationary Trolls in the duct entry and Lrolls in the rest of the duct (Figure 4(h)). This specific flow pattern was predicted by a linear stability analysis from Cheng and Wu (1976). And the T-rolls and L-rolls can merge together to form U-rolls (Figure 4(g)).

Other mixed vortex flow patterns were revealed from weak nonlinear analyses based on the competition between the longitudinal and transverse disturbances in the flow (Brand et al. 1991 and Müller et al., 1993). They reported that the mixed patterns could be in the forms of L-rolls in the upstream and Trolls in the downstream, Trolls in the upstream and Lrolls in the downstream, and T-rolls in the entry and exit sections of the duct and L-rolls in the middle, depending on the Reynolds number of the flow.

3. Formation of vortex rolls

It is of interest to understand how the regular vortex rolls examined above are formed under the action of buoyancy. This was investigated by Chang et al. (1997) both experimentally and numerically. Specifically, they first imposed a fully developed flow of air in the duct ($A=12$) and a subcritical temperature difference between the top and bottom plates for a sufficiently long period of time so that the flow was at a highly subcritical state and therefore unidirectional. Then, the Rayleigh number of the flow was raised to the required supercritical level and the subsequent evolution of the vortex flow patterns was visualized. They noted that the formation of the longitudinal vortex flow was rather simple and began with the generation of a pair of Lrolls near the two duct sides and the ensuing generation of Trolls near the exiting ones. However, the formation of the transverse vortex flow prevailed at lower

Reynolds numbers is much more complicate and is shown in Figure 7. The results indicate that shortly after the Rayleigh number is raised, rolls appear near the duct sides (Figure 7(b)). Slightly later, T-rolls are repeatedly generated in the duct entry and in the mean time more L-rolls are induced (Figure 7(c)). As time proceeds, L-rolls and T-rolls grow in size and intensity, and they merge together to form somewhat distorted rolls (Figure 7(d)). Meanwhile, the rolls are pushed by the mean flow to move slowly downstream (Figure 7(e)). Then, it takes certain amount of time for the distorted rolls to move out of the duct and the T-rolls in the entry half of the duct become regular in shape (Figure 7(f)-(h)). Finally, a pure transverse vortex flow is formed in the duct. The above evolution processes leading the transverse vortex flow suggest the importance of the competition between the L-rolls and T-rolls in determining the final vortex flow patterns. At a low Re the T-rolls predominate over the L-rolls and we eventually have transverse flow in the duct. At slightly higher Re the L-rolls and T-rolls can be at comparable strength and one cannot dominate over another. As a result, a mixed vortex flow appears in the duct.

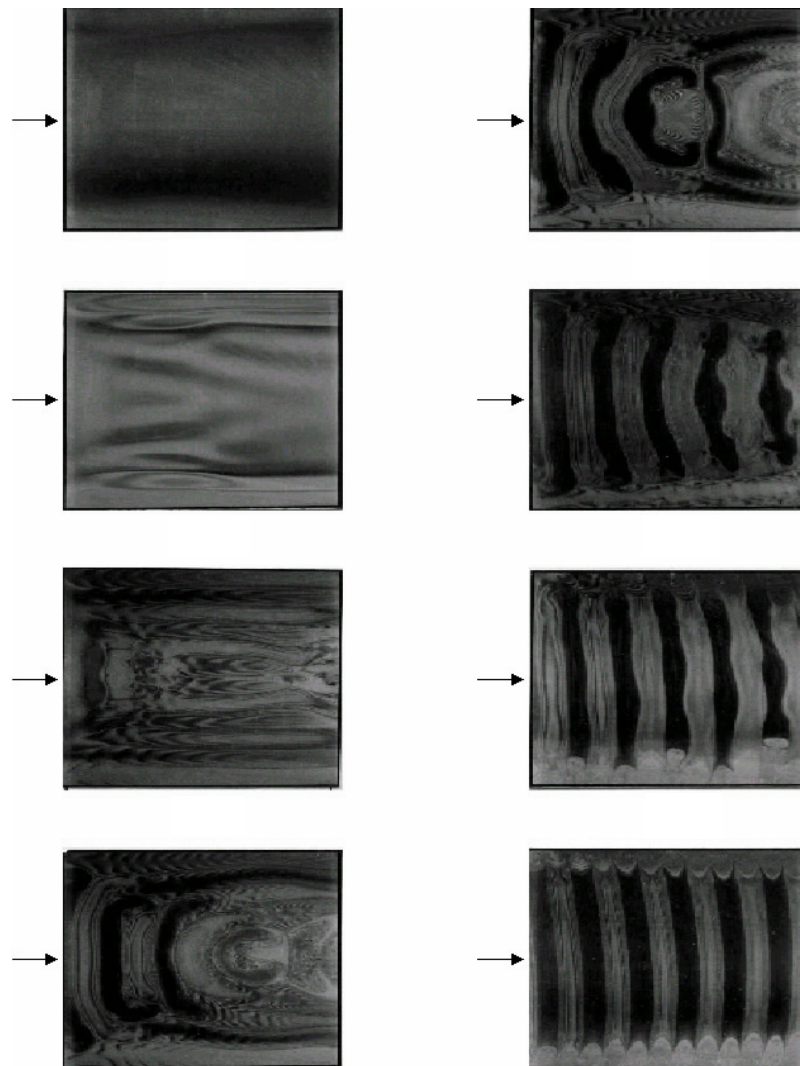


Fig.7. Flow pattern formation from the unidirectional flow to the transverse rolls by raising Ra from 1,500 to 4,300 in 110 s at Ra =5 and t = (a) 0 s, (b) 33 s, (c) 60 s, (d) 87 s, (e) 101 s, (f) 154 s, (g) 530 s and (h) 600 s for air with $A=12$.

4. Aspect ratio effects

It is readily realized that the duct aspect ratio can have profound influence on the buoyancy driven vortex flow, in view of the viscous damping effects associated with the sidewalls of the duct and the lateral space available for the vortex flow to move depend very much on the

aspect ratio. Moffat and Jensen (1986) did suggest that the vortex flow was sensitive to the aspect ratio. A recent three-dimensional linear stability analysis from Nicolas et al. (2000) provided detailed results for the effects of the aspect ratio on various vortex flow characteristics near the convective thresholds. They showed that the critical Rayleigh number for the onset of L-rolls increased substantially with the reduction in the aspect ratio. Similar trends were noted for the onset of the T-rolls. Besides, they also provided the data for the size and convection speed of the rolls. Their results clearly suggest that the higher viscous damping of the sidewalls for a narrower duct produces stabilizing effects for the vortex flow. This indeed was experimentally noted by Chang and Lin (1998) in examining the effects of the aspect ratio on the longitudinal vortex flow. They found that the flow was stabler for a lower aspect ratio. Moreover, for $A \leq 6$ the transition of the flow from steady to time-dependent states at increasing buoyancy-to-inertia ratio was found to be supercritical, signifying the presence of a finite Gr/R range for the existence of a time periodic vortex flow. At the periodic state axially snaking longitudinal rolls prevail in the duct. The recent study from Jiang (2000), however, revealed that the mixed vortex flow like Figure 4(b) became highly unstable in a duct with an intermediate aspect ratio for A around 6. This very different trend is attributed to the observation that the downstream traveling T-rolls in the duct core have too small spanwise space to move comfortably for the aspect ratio $A \leq 6$ and they become rather distorted and highly unstable.

Because of its relevance to the growth of thin films from the CVD processes, the characteristics of the longitudinal vortex flow of gas in a lower aspect ratio duct were numerically and experimentally explored (Abou-Ellail and Morcos, 1983, Moffat and Jensen, 1986, Ouazzani and Rosenberger, 1990, Nyce et al., 1992, Evans and Grief, 1993, Cheng and Shi, 1994, Narusawa, 1995, Chen and Lavine, 1996 and Spall, 1996). The results from these studies all indicate that the detailed characteristics of the L-rolls depend substantially on the aspect ratio. The effects of the duct aspect ratio on the transverse vortex flow, however, are less studied.

5. Vortex flow stabilization

The presence of unstable irregular vortex flow driven at a high buoyancy-to-inertia ratio is unwelcome in MOCVD processes. Methods such as tilting and/or rotating the substrates in MOCVD reactors have been used in industry for some time. The acceleration of the main gas flow through the substrate tilting indeed can regularize and even eliminate the unstable flow and reduce the boundary layer growth over the substrate at low to intermediate buoyancy. At high buoyancy the substrate tilting can still effectively and completely wipe out the regular temporal flow oscillation (Tseng et al., 2000). But the vortex flow can only be weakened to some degree. Besides, more vortex rolls can be induced in the second half of the plate tapering duct due to the continuing increase of the duct aspect ratio in the mean flow direction.

It is noted that the stabilization of the buoyancy driven unstable vortex flow in the horizontal channel by rotating the substrate has not been investigated to any significant detail based on careful experimental measurement and/or numerical simulation. However, the vortex flow stabilization through heating the top plate of the duct has received some attention. The thermally stable stratification of the flow near the heated top plate was demonstrated to be effective in stabilizing the vortex flow driven by the heated bottom plate (Akiyama et al., 1971, Incropera and Schutt, 1985, Maughan and Incropera, 1990b, and Ingham et al., 1995). A recent flow visualization experiment from Chang (2001) clearly showed that heating the top plate to a certain uniform level could completely suppress the unstable irregular vortex air flow and the flow became steady and unidirectional.

Another stabilization method again through the acceleration of the main flow by placing a

surface mounted rectangular block of various sizes and orientations on the bottom plate of the channel was recently attempted by Shu (2001). His result disclosed that mounting a slender block at the inlet of the channel with its long sides normal to the forced flow direction could stabilize the transverse and mixed vortex flows of air in the region directly behind the block. Particularly, the temporal flow oscillation can be effectively suppressed. Moreover, the stabilization of the vortex flow can be enhanced considerably by increasing the length and height of the block.

6. Vortex flow over a circular heated plate

In an actual horizontal MOCVD reactor, the vapor is forced to flow over a high temperature circular wafer upon which thin crystal films are grown. It is reasonable to expect that to a certain degree the vortex flow driven by the circular heated surface is different from that driven by the rectangular one which has been extensively studied over the past and examined in the above section. In-depth analyses are needed to unravel the detailed vortex flow characteristics under such situation.

The vortex air flow patterns driven by a 12-in circular heated plate embedded in the bottom of a horizontal flat duct ($A=20$) were recently visualized by our research and are illustrated in Figure 8. The induced steady longitudinal vortex flow revealed from the top view flow photo given in Figure 8(a) clearly indicates that the onset locations of the rolls driven by the circular plate are very different from those induced by the rectangular plate (Figure 4(c)). Specifically, for the circular plate the L-rolls are initiated earlier in the duct core. This is completely opposite to the situation for the rectangular plate. Besides, the circular geometry of the plate to some degree tends to break the spanwise symmetry of the flow. This is attributed to the fact that the buoyancy induced thermals on the plate preceding the generation of L-rolls are slightly unstable. The T-rolls shown in Figure 8(b) indicate that the rolls get bigger as they slowly move downstream. In addition, an incomplete circular roll is induced right around the edge of the circular plate. The roll does not surround the entire periphery of the plate. Moreover, the T-rolls do not travel downstream at a constant speed.

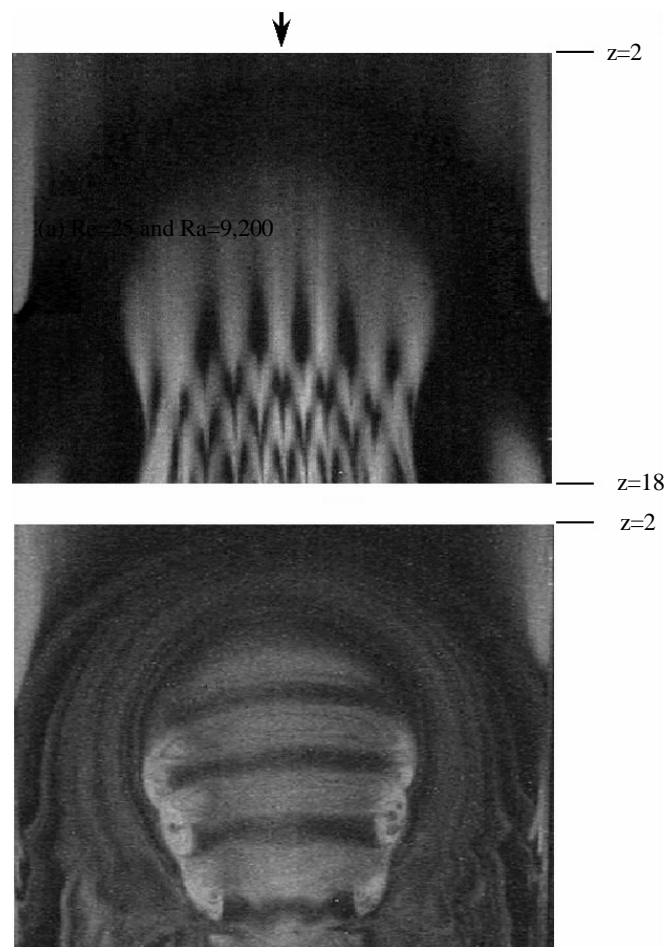


Fig. 8 Top view flow photos for (a) steady longitudinal rolls and (b) moving transverse rolls induced by circular heated plate for air flow in a duct with $A=20$

7. Concluding remarks and directions for future research

Over the past two decades significant advances have been made both qualitatively and quantitatively in the understanding of the low Reynolds number mixed convective buoyancy driven vortex flow and associated heat transfer characteristics in horizontal plane channels heated uniformly from below. Several new vortex flow patterns were unveiled. However, careful and in-depth studies are still needed in view of the recent technological applications associated with the thin film growth from the horizontal MOCVD processes. Research needs in the near future based on my personal speculation are briefly summarized in the following.

- (1). Detailed analyses are required to unravel various aspects of the mixed convective vortex gas flow over a heated circular plate, including the possible vortex flow patterns, flow regime map, and return flow.
- (2). Methods to stabilize the unstable vortex flow driven at high buoyancy-inertia ratios need to be developed and investigated in detail. In particular, how the wafer tilting and/or rotation, duct wall tapering, and thermal and flow boundary modifications affect the temporal and spatial vortex flow characteristics should be examined.
- (3). The presence of the return flow produces “memory effects” in the MOCVD processes and has to be eliminated. Methods to eliminate the return flow are therefore highly needed.
- (4). Eventually, we will face the challenge of finding an optimal duct geometry imposed with some suitable flow and thermal boundary conditions so that the velocity, temperature and concentration boundary layers over the wafer are of uniform thickness at high Gr^2/Re . Moreover, the system should be able to operate at a wide pressure range.

Acknowledgement

The multi-year financial support of this study on the vortex flow and heat transfer in channels by the engineering division of the National Science Council of Taiwan, R.O.C. through the contracts NSC 81-0404-E-009-101, NSC 82-0404-E-009-141, NSC 83-0404-E-009-054, NSC 85-2212-E-009-031, NSC 87-2218-E-009-006, NSC 88-2212-E-009-008, and NSC 89-2212-E-009-014 is greatly acknowledged.

References

- M. M. M. Abo-Elail and S. M. Morcos, Buoyancy effects in the entrance region of horizontal rectangular channels, ASME, J. Heat Transfer, vol. 105, pp. 924 -928, 1983.
- M. Akiyama, G. J. Hwang and K. C. Cheng, Experiments on the onset of longitudinal vortices in laminar forced convection between horizontal plates, ASME, J. Heat Transfer, vol.93, pp.335-341, 1971.
- H. R. Brand, R. J. Dessler, and G. Ahlers, Simple model for the Bénard instability with horizontal flow near threshold, Phys. Rev. A, vol. 43, no. 8, pp. 4362-4368, 1991.
- C Y. Chang, Effects of Top Plate Heating on Mixed Convection Vortex Flow of Air in a Bottom Heated Horizontal Flat Duct, M.S. thesis, National Chiao Tung University, Hsinchu, Taiwan, 2001.
- M. Y. Chang and T. F. Lin, Vortex flow pattern selection and temporal-spatial structures of transverse and mixed vortex rolls in mixed convection of air in a horizontal flat duct, Phys. Rev. E, vol. 54, pp. 5146-5160, 1996.
- M. Y. Chang and T. F. Lin, Experimental study of aspect ratio effects on longitudinal vortex flow in mixed convection of air in a horizontal rectangular duct, Int. J. Heat Mass Transfer, vol. 41, nos. 4-5, pp. 719-733, 1998.
- M. Y. Chang, C. H. Yu and T. F. Lin, Changes of longitudinal vortex roll structure in a mixed convective air flow through a horizontal plane channel: An experimental study, Int. J. Heat Mass

- Transfer, vol. 40, no. 2, pp. 347-363, 1997a.
- M. Y. Chang, C. H. Yu and T. F. Lin, Flow visualization and numerical simulation of transverse and mixed vortex roll formation in mixed convection of air in a horizontal flat duct, *Int. J. Heat Mass Transfer*, vol. 40, no. 8, pp. 1907-1922, 1997b.
- S. S. Chen and A. S. Lavine, Laminar, buoyancy induced flow structures in a bottom heated, aspect ratio 2 duct with throughflow, *Int. J. Heat Mass Transfer*, vol. 39, no. 1, pp. 1-11, 1996.
- T. C. Cheng, J. T. Lir and T. F. Lin, Stationary transverse rolls and vortices in limiting low Reynolds number mixed convective air flow near the convective threshold in a horizontal flat duct, *Int. J. Heat Mass transfer*, in press, 2001
- K. C. Cheng and Lei Shi, Visualization of convective instability phenomena in the entrance region of a horizontal rectangular channel heated from below and/or cooled from above, *Experimental Heat Transfer*, vol. 7, pp. 235-248, 1994.
- K. C. Cheng and R. S. Wu, Axial heat conduction effects on thermal stability of horizontal plane Poiseuille flows heated from below, *ASME, J. Heat Transfer*, pp. 564-569, 1976.
- K. C. Chiu and F. Rosenberger, Mixed convection between horizontal plates – I. Entrance effects, *Int. J. Heat Mass Transfer*, vol. 30, pp. 1645-1654, 1987.
- G. Evans & R. Greif, Thermally unstable convection with applications to chemical vapor deposition channel reactors, *Int. J. Heat Mass Transfer*, vol. 36, no. 11, pp. 2769-2781, 1993.
- K. Fukui, M. Nakajima and H. Ueda, The longitudinal vortex and its effects on the transport processes in combined free and forced laminar convection between horizontal and inclined parallel plates, *Int. J. Heat Mass Transfer*, vol. 26, pp. 109-120, 1983.
- M. L. Hitchman, K. F. Jensen, *Chemical Vapor Deposition Principles and Applications*, Academic Press, San Diego, 1993 (Chapter 2).
- G. J. Hwang and K. C. Cheng, Convective instability in the thermal entrance region of a horizontal parallel-plate channel heated from below, *ASME, J. Heat Transfer*, vol. 95, pp. 72-77, 1973.
- G. J. Hwang and C. L. Liu, An experimental study of convective instability in the thermal entrance region of a horizontal parallel-plate channel heated from below, *Can. J. Chem. Eng.* vol. 54, pp. 521-525, 1976.
- F. P. Incropera and J. A. Schutt, Numerical simulation of laminar mixed convection in the entrance region of horizontal rectangular ducts, *Num. Heat Transfer*, vol. 8, pp. 707-729, 1985.
- D. B. Ingham, P. Watson, and P. J. Heggs, Recirculating laminar mixed convection in a horizontal parallel plate duct, *Int. J. Heat and Fluid Flow*, vol. 16, no. 3, pp. 202-210, 1995.
- N. K. Ingle and T. J. Mountziaris, The onset of transverse recirculations during flow of gases in horizontal ducts with differentially heated lower walls, *J. Fluid Mech.*, vol. 277, pp. 249-269, 1994.
- H. J. Jiang, *Vortex Flow Structures in Mixed Convective Air Flow through a Bottom Heated Horizontal Rectangular Duct: Effects of Aspect Ratio*, MS. thesis, National Chiao Tung University Hsinchu, Taiwan, 2000.
- Y. Kamotani and S. Ostrach, Effect of thermal instability on thermally developing laminar channel flow, *ASME, J. Heat Transfer*, vol. 98, pp. 62-66, 1976.
- Y. Kamotani, S. Ostrach and H. Miao, Convective heat transfer augmentation in thermal entrance regions by means of thermal instability, *ASME, J. Heat Transfer*, vol. 101, pp. 222-226, 1979.
- J. T. Lir, M. Y. Chang and T. F. Lin, Vortex flow patterns near critical state for onset of convection in air flow through a bottom heated horizontal flat duct, *Int. J. Heat Mass Transfer*, vol. 44, pp. 705-719, 2001.
- J. M. Luijckx, J. K. Platten and J. C. Legros, On the existence of thermoconvective rolls, transverse to a superimposed mean Poiseuille flow, *Int. J. Heat Mass Transfer*, vol. 24, no. 7, pp. 1287-1291, 1981.
- J. M. Luijckx, J. K. Platten and J. Crokney, Precise measurements of wavelength at onset of Rayleigh-Bénard convection in a long rectangular duct, *Int. J. Heat Mass Transfer*, vol. 25, no. 8, pp. 1252-1254, 1982.
- T. M. Makhviladze and A. V. Martjushenko, Several aspects of the return flows formation in horizontal CVD reactors, *Int. J. Heat Mass Transfer*, vol. 41, no. 16, pp. 2529-2536, 1998.
- J. R. Maughan and F. P. Incropera, Fully developed mixed convection in a horizontal channel heated uniformly from above and below, *Num. Heat Transfer A*, vol. 17, pp. 417-430, 1990a.

- J. R. Maughan and F. P. Incropera, Regions of heat transfer enhancement for laminar mixed convection in a parallel plate channel, *Int. J. Heat Mass Transfer*, vol. 33, no. 3, pp. 555-570, 1990b.
- K. Moffat and K. F. Jensen, Complex flow phenomena in MOCVD reactors, *J. Crystal Growth*, vol. 77, pp. 108-119, 1986.
- H. W. Müller and M. Lücke and M. Kamps, Transversal convection patterns in horizontal shear flow, *Phys. Rev. A*, vol. 45, no. 6, pp. 3714-3726, 1992.
- H. W. Müller, M. Tveitereid and S. Trainoff, Rayleigh-Bénard problem with imposed weak through-flow: Two coupled Ginzburg-Landau equations, *Phys. Rev. E*, vol. 48, no.1, pp. 263-272, 1993.
- U. Narusawa, Numerical analysis of mixed convection at the entrance region of a rectangular duct heated from below, *Int. J. Heat Mass Transfer*, vol. 36, no. 9, pp. 2375-2384, 1993.
- U. Narusawa, Buoyancy-induced laminar convective rolls in rectangular geometry, *Num. Heat Transfer, Part A*, vol. 28, pp. 195-213, 1995.
- X. Nicolas, J. M. Luijckx, and J. K. Platen, Linear stability of mixed convection flows in horizontal rectangular channels finite transversal extension heated from below, *Int. J. Heat Mass Transfer*, vol. 43, pp.589-610, 2000.
- T. A. Nyce, J. Ouazzani, A. Durand, Durbin and F. Rosenberger, Mixed convection in a horizontal rectangular channel-experimental and numerical velocity distributions, *Int. J. Heat Mass Transfer* vol. 35, no. 6, pp. 1481-1494, 1992.
- S. Ostrach and Y. Kamotani, Heat transfer augmentation in laminar fully developed channel flow by means of heating from below, *ASME, J. Heat Transfer*, vol. 97, pp. 220-225, 1975.
- M. T. Ouazzani, J. P. Caltagirone, G. Meyer and A. Mojtabi, Etude numérique et expérimentale de la convection mixte entre deux plans horizontaux, *Int. J. Heat Mass Transfer*, vol. 32, pp. 261-269, 1989.
- J. Ouazzani and F. Rosenberger, Three-dimensional modeling of horizontal chemical vapor deposition: I MOVCD at atmospheric pressure, *J. of Crystal Growth*, vol. 100, pp. 545-576, 1990.
- D. S. Shu, Buoyancy Driven Vortex Flow Patterns in Mixed Convection of Air through a Blocked Horizontal Flat Duct Heated from below, MS. thesis, National Chiao Tung University Hsinchu, Taiwan, 2001.
- R. E. Spall, Observations of spanwise symmetry breaking for unsteady mixed convection in horizontal ducts, *ASME, J. Heat Transfer*, vol. 118, pp. 885-888, 1996.
- W. S. Tseng, W. L. Lin, C. P. Yin, C. L. Lin and T. F. Lin, Stabilization of buoyancy driven unstable vortex flow in mixed convection of air in a rectangular duct by tapering its top plate, *ASME, J. Heat Transfer*, vol. 122, pp. 58-65, 2000.
- M. Tveitereid, H. W. Müller, Pattern selection at the onset of Rayleigh-Bénard convection in a horizontal shear flow, *Phys. Rev. E*, vol. 50, pp. 1219 -1226, 1994.
- E. P. Visser, C. R. Kleijn, C. A. M. Gorvart, C. J. Hoogendoorn, and L. J. Giling, Return flows in horizontal MOCVD reactors studied with the use of Particle injection and numerical calculations, *J. Crystal Growth*, vol. 94, pp.929-946, 1989.
- C. H. Yu, M. Y. Chang, C. C. Huang and T. F. Lin, Steady vortex roll structures in a mixed convective air flow through a horizontal plane channel: A numerical study, *Int. J. Heat Mass Transfer*, vol. 40, no. 3, pp. 505-518, 1997a.
- C. H. Yu, M. Y. Chang and T. F. Lin, Structures of moving transverse and tilted rolls in mixed convection of air in a horizontal plane channel, *Int. J. Heat Mass Transfer*, vol. 40, no. 2, pp. 333-346, 1997b.